Springer

KSME

Journal of Mechanical Science and Technology 30 (8) (2016) 3433~3440
www.springerlink.com/content/1738-494x(Print)/1976-3824(Online)
DOI 10.1007/s12206-016-0701-9

Optimum path-tracking control for inverse problem of vehicle handling dynamics†

Yingjie Liu* and Junsheng Jiang

School of Mechanical-Electronic and Vehicle Engineering, Weifang University, Weifang 261061, Shandong, China

(Manuscript Received September 16, 2014; Revised January 5, 2016; Accepted April 11, 2016)

Abstract

A method based on optimal control theory is presented in this paper to solve path-tracking problems in inverse vehicle handling dynamics. The idea behind is to identify the optimal steering torque input along a prescribed path to generate an expected trajectory that guarantees minimum clearance. Based on this purpose, the path-tracking problem, treated as an optimal control problem, is first converted into a nonlinear programming problem by Gauss pseudospectral method (GPM) and is then solved with Sequential quadratic programming (SQP). Finally, a real vehicle test is executed to verify the rationality of the proposed model and methodology. Results show that the minimum lateral position error of the generated path-tracking trajectory can be a good solution for path-tracking problem in inverse vehicle handling dynamics for GPM. The algorithm has higher calculation accuracy compared with other methods to solve path-tracking problems. The study could help drivers identify safe lane-keeping trajectories and areas easily.

Keywords: Vehicle handling dynamics; Path-tracking; Optimum control; Inverse problem

1. Introduction

Human driving characteristics are complex combinations of physical and mental processes in response to perceived motion, visual, and acoustic cues. With different motion perceptions, drivers perform as a controller to satisfy key guidance and control requirements for vehicle system [1].

The growing mobility of people and goods has a significantly high societal cost. Several studies show that drivers are responsible for most accidents, which occur mainly due to distraction, and wrong perception and judgment of the traffic and environmental situations around vehicles [2].

The study of inverse vehicle handling dynamics plays an important role in stability research, with advantage of ignoring the driver model. Thus, the study of inverse vehicle handling dynamics is proposed in this paper.

The general path-tracking control for inverse problem of vehicle handling dynamics scenario is shown in Fig. 1, where a vehicle travels along a prescribed path. The vehicle is expected to generate trajectory with minimum lateral distance error while tracking the prescribed path. Then, the optimal steering torque, steering rate, and as yaw rate are calculated.

A brief review of path-tracking problems in literatures is presented in this section.

Toshihiro et al. [3] proposed an automatic path-tracking controller of a four-wheel steering (4WS) vehicle based on the sliding mode control theory.

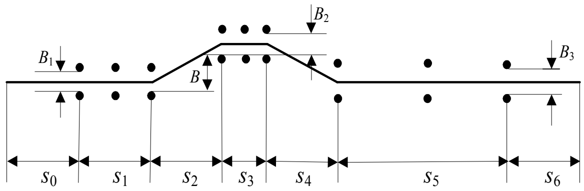

Fig. 1. Double lane change test road (● stands for stake).

Bektache et al. [4] developed a module that focused on the estimation of vehicle parameters, such as speed, direction, and position, using a kinematic model of each vehicle to generate trajectory estimations.

Ju [5] proposed a Linear-matrix-inequality (LMI)-based H ∞ control algorithm and utilized the fusion of look-ahead and look-down sensors to solve lateral control problems of autonomous vehicles.

Kim et al. [6] utilized a Model predictive controller (MPC) method to solve path-tracking problems of autonomous vehicles. Calculation results indicate that the proposed MPC structure better matches the target criteria.

Taehyun et al. [7] described a development of a collision avoidance controller for autonomous vehicles to track the desired collision avoidance path. Simulation results confirm that the control system can perform collision-free maneuvers effectively.

Xu et al. [8] proposed a pedestrian localization method

*Corresponding author. Tel.: +86 18253677382, Fax.: +86 536 8797126
E-mail address: ufoliuyingjie@163.com
† Recommended by Associate Editor Deok Jin Lee
© KSME & Springer 2016

based on extended Kalman filter to estimate the possibility of pedestrian-vehicle collision, which includes collision prediction, pedestrian detection, and localization.

Anderson et al. [9] described a method to deal with semi-autonomous hazard avoidance problems in the presence of unknown moving obstacles and unpredictable driver inputs. The method was used to predict the motion and to anticipate intersection of the host vehicle with both static and dynamic hazards, excluding projected collision states from a traversable corridor.

Amir et al. [10] presented a non-linear adaptive dynamic surface sliding control method for a simultaneous vehicle-handling and path-tracking improvement.

Xu et al. [11] developed a receding-horizon formulation that reduced the overall burden of path-planning computations and made it suitable for highly large domains.

Ghaffari et al. [12] selected lane change maneuver as the object behavior and proposed novel, adaptive neuro-fuzzy inference models. The models were able to simulate and predict the behavior of a driver-vehicle-unit in a lane change maneuver for various time delays.

Jin et al. [13] redefined the equation of Time-to-collision (TTC) using visual angle information, taking lateral separation into account.

The Gauss pseudospectral method in its current form is one of the newest numerical approaches in today's literature [14], although it bears resemblance to work done in 1979 [15]. The method has the potential of solving real-time optimal control problems with fewer parameters and higher accuracy advantages [16, 17].

This paper aims to present a method based on optimal control theory for path-tracking problems in inverse vehicle handling dynamics. The method is used to calculate optimal control input, such as steering torque for driving in a desired path without striking neighboring obstacles or deviating from the prescribed path. The rest of the paper is organized as follows: Sec. 2 presents the model of vehicle path-tracking problem; Sec. 3 presents the solution for the proposed model; Sec. 4 illustrates the numerical simulation and experimental verification; and Sec. 5 summarizes the conclusions and suggests future research directions.

2. Model of vehicle path-tracking problem

2.1 Mathematical model of vehicle path-tracking problem

The longitudinal force acting on the front wheels is assumed to be small. The influence on the tire cornering characteristics affected by ground tangential force is ignored within linear range. The vehicle movement can be simplified as a 4-DOF vehicle model, depicted in Fig. 2. The vehicle model has the following rotary motion of the steering system, longitudinal and lateral motion and yawing motion degree-of-freedom. The main model composed by the rotary motion of the steering system, the lateral and longitudinal motion, and the yawing motion can be manifested in the simplified model. Thus, the model has greater practical significance for theoretical analysis. In state space form, it is:

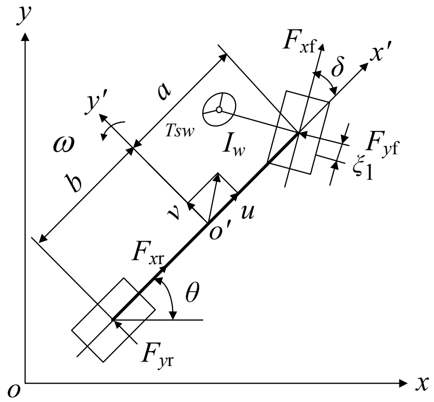

Fig. 2. 4-DOF vehicle model.

$$\begin{cases} \dot{u} = v\omega + \dfrac{F_{xf}\cos\delta - F_{yf}\sin\delta + F_{xr} - F_{f} - F_{w}}{m} \\ \dot{v} = -u\omega + \dfrac{F_{yf}\cos\delta + F_{yr} + F_{xf}\sin\delta}{m} \\ \dot{\omega} = \dfrac{aF_{yf}\cos\delta - bF_{yr} + aF_{xf}\sin\delta}{I_z} \\ \dot{\delta} = p \\ \dot{p} = -\dfrac{k_1\xi_1}{I_w u}v - \dfrac{k_1\xi_1 a}{I_w u}\omega + \dfrac{(k_1\xi_1 - k_w)}{I_w}\delta - \dfrac{c_w}{I_w}p + \dfrac{T_{sw}i}{I_w} \end{cases} \tag{1}$$

where m is vehicle mass; I_z is moment of inertia around the z axis; v and u are lateral and longitudinal speed, respectively; ω is yaw rate of the vehicle, θ is heading angle of the vehicle, a and b are distances of front and rear axles from the center of gravity, respectively; I_w is moment of inertia of the steering system; i is transmission ratio of the steering system; ξ_1 is front wheel aligning arm of force; c_w is drag coefficient; T_{sw} is steering torque, and F_{yf} and F_{yr} are lateral forces of front and rear tires, respectively. In $F_f = mgf$, g is gravity acceleration and f is coefficient of rolling resistance. In $F_w = \dfrac{C_D A u^2}{21.15}$, C_D is coefficient of air resistance and A is frontal area. p is steering rate, F_{xf} and F_{xr} are the traction or brake forces of front and rear wheels, respectively, k_w is synthesized cornering stiffness, δ is front steering angle, and k_1 is synthesized stiffness of front tires.

Considering the effect of the traction/brake force, the lateral forces of the front and rear tires are:

$$\begin{cases} F_{yf} = k_1(\dfrac{v + a\omega}{u} - \delta)\sqrt{1 - (\dfrac{F_{xf}}{\mu F_{zf}})^2 + (\dfrac{F_{xf}}{k_1})^2} \\ F_{yr} = k_2(\dfrac{v - b\omega}{u})\sqrt{1 - (\dfrac{F_{xr}}{\mu F_{zr}})^2 + (\dfrac{F_{xr}}{k_2})^2} \end{cases} \tag{2}$$

where k_2 is synthesized stiffness of rear tires and μ is coefficient of friction.

Considering the longitudinal load transfer on the front axle and the rear one, the vertical forces of the front and rear wheels are:

$$\begin{cases} F_{zf} = \dfrac{mgb - (F_{xf} + F_{xr})h_g}{a+b} \\ F_{zr} = \dfrac{mga + (F_{xf} + F_{xr})h_g}{a+b} \end{cases} \tag{3}$$

where h_g is height of the center gravity.

The state variables are lateral and longitudinal velocity in the body frame, yaw rate, front steering angle, steering rate, lateral and longitudinal vehicle coordinates in the inertial frame, and heading angle.

To calculate the vehicle positions defined by x and y coordinates, the vehicle velocity in the body coordinate is projected as:

$$\begin{cases} \dot{x} = u\cos\theta - v\sin\theta \\ \dot{y} = v\cos\theta + u\sin\theta \end{cases}. \tag{4}$$

According to Eqs. (1) and (4), state equation can be described as:

$$\dot{\boldsymbol{x}} = f[\boldsymbol{x}(t), z(t)] \tag{5}$$

where $\boldsymbol{x}(t)$ and $z(t)$ are state and input, respectively, $\boldsymbol{x}(t) = [u(t), v(t), \omega(t), \delta(t), p(t), x(t), y(t), \theta(t)]^T$ $z(t) = [T_{sw}(t)]^T$.

2.2 Constrains

The initial and terminal states are described as:

$$\boldsymbol{x}(t_0) = [u_0, 0, 0, 0, 0, 0, 0, 0]^T \tag{6}$$

$$[x_2(t_f), x_3(t_f), x_4(t_f), x_5(t_f), x_8(t_f)]^T = [0,0,0,0,0]^T. \tag{7}$$

Since it is required that rollover should be avoided for the vehicle, the path constraint is imposed as [18]:

$$\frac{u^2\delta}{(a+b)(1+Ku^2)g} \le \frac{D}{2h_g} \tag{8}$$

where D is wheel base and K is stability factor.

When the vehicle is driven by the front wheels, the constraints on F_{xf} and F_{xr} are imposed as [19]:

$$\left.\begin{aligned} F_{xf} &\le \frac{\mu mgb}{a+b+\mu h_g} \\ F_{xr} &= 0 \end{aligned}\right\}. \tag{9}$$

When the brakes are applied to decelerate the vehicle and all the wheels are assumed in lock-brake, the constraints on F_{xf} and F_{xr} are as follows:

$$\left.\begin{aligned} F_{xf} &\ge -\frac{\mu mg(b+\mu h_g)}{a+b} \\ F_{xr} &= \frac{a-\mu h_g}{b+\mu h_g}F_{xf} \end{aligned}\right\}. \tag{10}$$

The boundary constraint of the control variable is decided by the driver's physiological limit as:

$$z_{\min} \le z \le z_{\max} \tag{11}$$

where $z_{\min}$ and $z_{\max}$ are the lower and upper limit values of the steering torque, respectively.

2.3 Optimal control object of path tracking problem

Vehicle path-tracking problem can be regarded as an optimal control problem. Lateral and longitudinal velocity in the body frame, yaw rate, front steering angle, steering rate, lateral and longitudinal vehicle coordinates in the inertial frame, and heading angle are determined as the state variables. Steering torque is set as the control variable. Minimum lateral distance error throughout the process of tracking the prescribed path is determined as control object.

The cost function is:

$$J(z) = \int_{t_0}^{t_f}\left((\frac{y-y_d}{\hat{E}})^2 + (\frac{z}{\hat{T}_{sw}})^2 \right)dt = \int_{t_0}^{t_f} L(\boldsymbol{x}, z, t)dt \tag{12}$$

where t_0 is initial time, t_f is final time, and y_d is prescribed path. $\hat{E}$ is standard threshold of lateral distance error of $y - y_d$, $\hat{E} = 0.3$ m. $\hat{T}_{sw}$ is standard threshold of the steering torque, $\hat{T}_{sw} = 8$ N · m.

The double lane change test road is described in Fig. 1 [19]. where $s_0 = s_1 = s_2 = s_4 = 2u$, $s_3 = u$, $s_5 = 5u$ and $s_6 = 3u$. B is the distance of lane-change, B = 3.5 m. B_1, B_2, and B_3 are distances between the stakes, B_1 = 1.1L+0.25 = 2.12 m, B_2 = 1.2L+0.25 = 2.29 m, B_3 = 1.3L+0.25 = 2.46 m, where L is width of the vehicle, L = 1.7 m.

3. GPM of solving vehicle path-tracking problem

For the sake of convenience, the path-tracking problem is transformed into a Bolza problem.

Bolza cost function is:

$$J = \psi(\boldsymbol{x}(t_0), t_0, \boldsymbol{x}(t_f), t_f) + \int_{t_0}^{t_f} g(\boldsymbol{x}(t), z(t), t)dt. \tag{13a}$$

The dynamic constrain is:

$$\dot{\boldsymbol{x}} = f(\boldsymbol{x}(t), z(t), t) \quad t \in [t_0, t_f]. \tag{13b}$$

The boundary constrain is:

$$\varphi(\boldsymbol{x}(t_0),t_0,\boldsymbol{x}(t_f),t_f)=\boldsymbol{0}. \tag{13c}$$

The inequality path constraint is:

$$C[\boldsymbol{x}(t),z(t),t]\le \boldsymbol{0} \quad t\in[t_0,t_f] \tag{13d}$$

where $\boldsymbol{x}(t)\in R^n$ is state and $z(t)\in R^m$ is input.

In Eqs. (13a)-(13d), functions ψ , g , f , φ and C are defined as follows:

$$\psi : R^n \times R \times R^n \times R \to R$$
$$g : R^n \times R^m \times R \to R$$
$$f : R^n \times R^m \times R \to R^n$$
$$\varphi : R^n \times R \times R^n \times R \to R^q$$
$$C : R^n \times R^m \times R \to R^c .$$

The main idea of the GMP algorithm is given as:

Step 1: Time discretization

The independent variable can be mapped to the general interval $\tau\in[-1,1]$ via affine transformation as [16]:

$$\tau = 2t/(t_f-t_0)-(t_f+t_0)/(t_f-t_0) \tag{14}$$

where $t\in[t_0,t_f]$.

Step 2: Approximating state and control variables

The state and control variables are approximated by different Lagrange interpolating polynomials $L_i(\tau)$ $(i=0,1,\cdots,N)$ and $L_i^*(\tau)$ $(i=0,1,\cdots,N)$ in each subinterval, where

$$L_i(\tau)=\prod_{j=0,j\ne i}^{N}\frac{\tau-\tau_j}{\tau_i-\tau_j} \tag{15}$$

$$L_i^*(\tau)=\prod_{j=1,j\ne i}^{N}\frac{\tau-\tau_j}{\tau_i-\tau_j}. \tag{16}$$

Step 3: Determining the constrain conditions

The kinematic differential equation constraint is converted by the algebraic constraint, and the terminal state constraint is solved by including an additional constraint.

Step 4: Solving the nonlinear programming problem.

3.1 Interval change

The minimization problem can be redefined by substituting Eq. (14) into Eqs. (13a)-(13d) as:

$$\min J=\psi(\boldsymbol{x}(-1),t_0,\boldsymbol{x}(1),t_f)+\frac{t_f-t_0}{2}\int_{-1}^{1}g(\boldsymbol{x}(\tau),z(\tau),\tau)d\tau \tag{17a}$$

$$\text{subject to}\quad \dot{\boldsymbol{x}}=\frac{t_f-t_0}{2}f(\boldsymbol{x}(\tau),z(\tau),\tau) \tag{17b}$$

$$\varphi(\boldsymbol{x}(-1),t_0,\boldsymbol{x}(1),t_f)=\boldsymbol{0} \tag{17c}$$

$$C[\boldsymbol{x}(\tau),z(\tau),\tau]\le\boldsymbol{0}. \tag{17d}$$

Problems in Eqs. (17a)-(17d) are referred to as the transformed continuous Bolza problem.

3.2 Global interpolation polynomial approximation of the state and control variables

The Gauss pseudospectral method, like Legendre and Chebyshev methods, is based on state and control trajectory approximations, using interpolating polynomials. The state is approximated using a basis of *N+1* Lagrange interpolating polynomials $L_i(\tau)$ as follows [14]:

$$\boldsymbol{x}(\tau)\approx \boldsymbol{X}(\tau)=\sum_{i=0}^{N}L_i(\tau)\boldsymbol{X}(\tau_i) \tag{18}$$

where $\mathbf{X}(\tau_i)=\mathbf{x}(\tau_i)$ and $(i=0,\cdots,N)$.

Additionally, the control is approximated using a basis of N Lagrange interpolating polynomials $L_i^*(\tau)$ $(i=0,1,\cdots,N)$ as:

$$z(\tau)\approx \boldsymbol{Z}(\tau)=\sum_{i=1}^{N}L_i^*(\tau)\boldsymbol{Z}(\tau_i) \tag{19}$$

where $\mathbf{Z}(\tau_i)=\mathbf{z}(\tau_i)$, $(i=0,\cdots,N)$.

It can be seen from Eqs. (15) and (16) that $L_i(\tau)(i=0,1,\cdots,N)$ and $L_i^*(\tau)(i=0,1,\cdots,N)$ satisfy the properties:

$$L_i(\tau_j)=\begin{cases}1, & i=j\\ 0, & i\ne j\end{cases}$$
$$L_i^*(\tau_j)=\begin{cases}1, & i=j\\ 0, & i\ne j\end{cases}.$$

3.3 The kinematic differential equation constraint converted by the algebraic constraint

Differentiating Eq. (18), Eq. (20) is expressed as:

$$\dot{\mathbf{x}}(\tau)\approx\dot{\mathbf{X}}(\tau)=\sum_{i=0}^{N}\dot{L}_i(\tau)\mathbf{X}(\tau_i)=\sum_{i=0}^{N}\mathbf{D}_{ki}\mathbf{X}(\tau_i). \tag{20}$$

The derivative of each Lagrange polynomial on Legendre-Gauss (LG) points can be represented in a differential approximation matrix, $\mathbf{D}_{ki}\in R^{N\times(N+1)}$. The elements of the differential approximation matrix are determined offline as follows:

$$\mathbf{D}_{ki}(\tau_k)=\dot{L}(\tau_k)=\begin{cases}\dfrac{(1+\tau_k)\dot{P}_N(\tau_k)+P_N(\tau_k)}{(\tau_k-\tau_i)\left[(1+\tau_i)\dot{P}_N(\tau_i)+P_N(\tau_i)\right]}, & i\ne k\\[2ex] \dfrac{(1+\tau_i)\ddot{P}_N(\tau_i)+2\dot{P}_N(\tau_i)}{2\left[(1+\tau_i)\dot{P}_N(\tau_i)+P_N(\tau_i)\right]}, & i=k\end{cases} \tag{21}$$

where $k=1,2,\cdots,N$ and $i=0,1,\cdots,N$.

The dynamic constraint is transcribed into algebraic constraints, using the differential approximation matrix as follows:

$$\sum_{i=0}^{N} \boldsymbol{D}_{ki}\boldsymbol{X}(\tau_i) - \frac{t_f - t_0}{2} f(\boldsymbol{X}(\tau_k), \boldsymbol{Z}(\tau_k), \tau_k; t_0, t_f) = \mathbf{0} . \quad (22)$$

3.4 The terminal state constraint in the discrete conditions

The set of nodes includes the N interior LG points, $\tau_1, \tau_2 \cdots, \tau_N$, the initial point, $\tau_0 \equiv -1$, and the final point $\tau_f \equiv 1$. Since $\boldsymbol{X}_f$ is absent in the state approximation, it must be controlled by including an additional constraint that relates the final state to the initial state via a Gauss quadrature to meet the state dynamic equation of Eq. (17b). According to the state dynamics:

$$\mathbf{x}(\tau_f) = \mathbf{x}(\tau_0) + \int_{-1}^{1} f(\mathbf{x}(\tau), \mathbf{z}(\tau), \tau) d\tau \quad (23)$$

which can be discretized and approximated as:

$$\boldsymbol{X}(\tau_f) = \mathbf{X}(\tau_0) + \frac{t_f - t_0}{2} \sum_{k=1}^{N} \omega_k f(\mathbf{X}(\tau_k), \mathbf{Z}(\tau_k), \tau_k; t_0, t_f) \quad (24)$$

where ω_k is Gauss weights.

$$\omega_k = \int_{-1}^{1} L_k(\tau)\, d\tau .$$

Next, Eq. (17c) is expressed as:

$$\varphi(\mathbf{X}(\tau_0), t_0, \mathbf{X}(\tau_f), t_f) = \mathbf{0} . \quad (25)$$

Furthermore, Eq. (17d) is evaluated at the LG points as:

$$C[\mathbf{X}(\tau_k), \mathbf{Z}(\tau_k), \tau_k; t_0, t_f] \le \mathbf{0} \quad (k = 1, \cdots, N) . \quad (26)$$

3.5 Calculating border control variables

Obtaining the accurate values of the border control variables is highly important. In the paper, they are solved by the method provided in Ref. [20].

3.6 Approximating performance index function

The integral term in the cost functional of Eq. (17a) can be approximated with a Gauss quadrature as before, resulting in:

$$J = \psi(\boldsymbol{X}_0, t_0, \boldsymbol{X}_f, t_f) + \frac{t_f - t_0}{2} \sum_{k=1}^{N} \omega_k g(\boldsymbol{X}_k, \boldsymbol{Z}_k, \tau_k; t_0, t_f) . \quad (27)$$

The optimal control problem of vehicle path tracking is defined as a nonlinear programming problem by the cost function of Eq. (27) and the algebraic constrains of Eqs. (22) and (24)-(26). The solution of the nonlinear programming problem is an approximate answer to the transformed continuous Bolza problem.

Table 1. Simulation parameters.

Parameter	Value
m/ kg	1265
I_z/ kg . m^2	1800
a/ m	1.170
b/ m	1.195
k_1/N . rad^{-1}	60042
k_2/N . rad^{-1}	109295
i	20
μ	0.8
I_w/ kg . m^2	16.38
c_w / (N · m · s · rad^{-1})	140
k_w / (N · m · rad^{-1})	0
ξ_1 / m	0.021
h_g/ m	0.53

Sequential quadratic programming (SQP) algorithm is used to solve the nonlinear programming problem [21].

SQP method solves the nonlinearly constrained problem by a sequence of Quadratic programming (QP) subproblems. It is assumed that an approximate solution x_k and a Lagrange multiplier vector λ_k are known when the k^{th} iteration starts. According to x_k and λ_k , the k^{th} QP subproblem P_k is obtained. Then, a new approximate solution x_{k+1} is attained by solving P_k and determining Lagrange multiplier vector correspondent λ_{k+1} . The process is repeated until the approximate optimal solution of the nonlinear programming problem is obtained.

4. Numerical simulation and experimental verification

4.1 Simulation result

Results of optimum path tracking of inverse problem of vehicle handling dynamics with the proposed method are confirmed by simulation. For the simulation, the calculation parameters are shown in Table 1.

The simulation conditions such as initial and final conditions and boundary constraint are shown in Table 2. The optimization is calculated by SQP algorithm and MATLAB software, using a 2.8 GHz/Pentium IV computer and Window XP operating system.

Realistically, drivers' ideal target trajectory should be a low-level, continuous and smooth curve. The double lane change test road is described as a third-order curve, where first-order derivative is continuous, transformed with cubic splines fitting shown in Fig. 3.

Fig. 3 shows the simulation result of the lateral distance while tracking the prescribed path. The figure indicates that

Table 2. Simulation conditions.

	Initial conditions	Final conditions		Boundary constraint
u (km/h)	105		$z_{\min}$ $(\mathrm{N\cdot m})$	-8
v (km/h)	0	0	$z_{\max}$ $(\mathrm{N\cdot m})$	8
ω (rad/s)	0	0		
p (°/s)	0	0		
x (m)	0			
y (m)	0			
θ (°)	0	0		

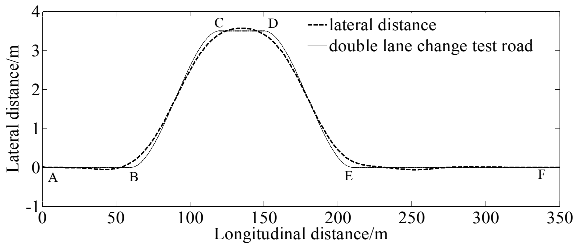

Fig. 3. Lateral distance.

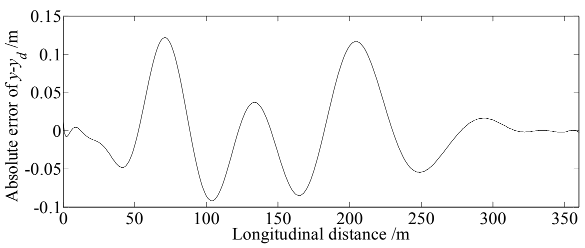

Fig. 4. Absolute error of y- y_d .

the vehicle can track the double lane change test road well with an initial speed of 105 km/h.

Fig. 4 describes the calculation result of the absolute error between the simulation result of the lateral distance and the prescribed path. It shows that the maximum value of the absolute error is about 0.12 m. The absolute error calculated with optimum control method is very small. Thus, the vehicle can travel along the prescribed trajectory with good tracking performance under optimum control condition.

Fig. 5 shows the result of the steering torque with different longitudinal distance. It shows that the steering torque has peak values at 60 m, 100 m, 150 m and 190 m, which indicates the hard sledding for the driver to manipulate the car.

Fig. 6 describes the calculation result of the steering rate. From the figure it is shown that the steering rate has bigger response values at 75 m and 210 m, which indicates the higher busyness degree for the driver to manipulate the car.

4.2 Evaluation of calculation accuracy

To compare the calculation accuracy of GPM with the numerical integration algorithm, the control variable obtained by calculating GPM algorithm is substituted into Eq. (1). Then,

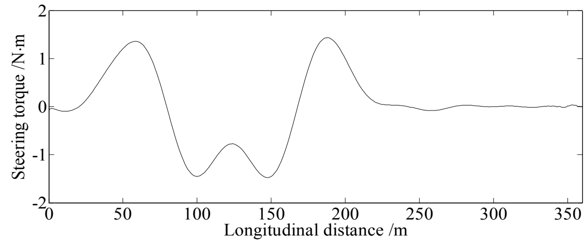

Fig. 5. Steering torque.

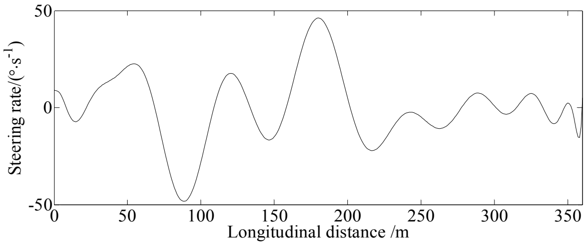

Fig. 6. Steering rate.

another optimal trajectory is calculated by the numerical integration algorithm. Finally, the absolute error between the results of the two optimal trajectories, which are calculated by the numerical integration algorithm and GPM algorithm respectively, and the result of the prescribed path are acquired. It is shown that the maximum value of the absolute error given by the calculation of GPM is about 0.12 m. However, the same value given by the calculation of the numerical integration algorithm is about 0.21 m. Thus, the solution used has a higher accuracy advantage in GPM algorithm compared with other traditional methods in solving path-tracking problems .

4.3 Experimental result

4.3.1 Test objectives

The ground test is conducted to obtain the related test data such as lateral distance and steering torque, with the purpose of verifying the feasibility of the simulation results.

4.3.2 Test ground and conditions

The overall length of the ground is 2212 m. At each end of the ground, the U-turn ring has a radius of 36 m. The longitudinal and lateral slopes of the ground are less than 2%. In order to satisfy the experimental conditions, the wind velocity must be less than 5 m/s, and the ambient temperature should be between 0°C and 40°C.

4.3.3 Block diagram of test system and measurement equipments

The block diagram of test system is shown in Fig. 7.

The measurement equipment is described as follows:

(1) RACELOGIC VBOX speed instrument, which is used to measure the vehicle speed precisely, is shown in Fig. 8(a);

(2) Steering torque/angle tester, which is used to measure the steering torque or the steering angle, is shown in Fig. 8(b);

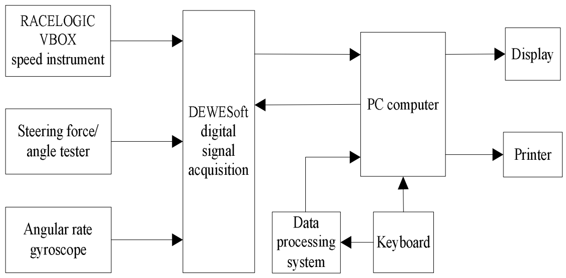

Fig. 7. Block diagram of test system.

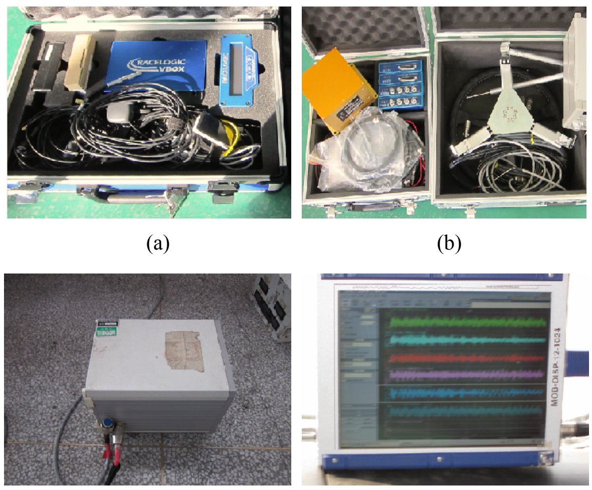

(a) (b) (c) (d)

Fig. 8. Measurement equipments: (a) RACELOGIC VBOX speed instrument; (b) steering torque/angle tester; (c) angular rate gyroscope; (d) DEWESoft digital signal acquisition.

(3) Angular rate gyroscope, which is used to measure the yaw rate and the lateral and longitudinal acceleration, is shown in Fig. 8(c);

(4) DEWESoft digital signal acquisition, which is used to collect and record different types of data simultaneously, is shown in Fig. 8(d);

(5) Other auxiliary equipment, such as stopwatch, battery, and wire, are also required for the test.

4.3.4 Test procedure

The test procedure in accordance with ISO/TR3888-1999 is as follows:

Step 1: As shown in Fig. 1, stakes are arranged and a prescribed path is painted exactly on the ground according to the double lane change test road (solid line shown in Fig. 3).

Step 2: Equipment shown in Fig. 7 is warmed up to normal operating temperature.

Step 3: A water injector is installed at the center of the front axle to record the real travelling trajectory in the form of water trace. With an initial velocity of 105 km/h, the tested vehicle travels along the initial lane, which is marked as the solid line AB shown in Fig. 3. At the same time, the water injector is opened to report the vehicle trajectory. A rapid lane change maneuver is implemented, which is marked as the solid line CD shown in Fig. 3. As the vehicle returns to the initial lane quickly and without touching any part of the stakes, a solid line EF shown in Fig. 3 is marked. The time history curves of the measured variables are recorded.

Step 4: Step 3 is repeated 12 times.

The test values are shown in Figs. 9(a)-(c). Figs. 9(a)-(c) shows errors between simulation value and experimental value caused by the subjective feeling and driving skill of the driver. However, the trend of the simulation value is similar with the experimental value, verifying the accuracy of the optimal control model and the feasibility of simulation results.

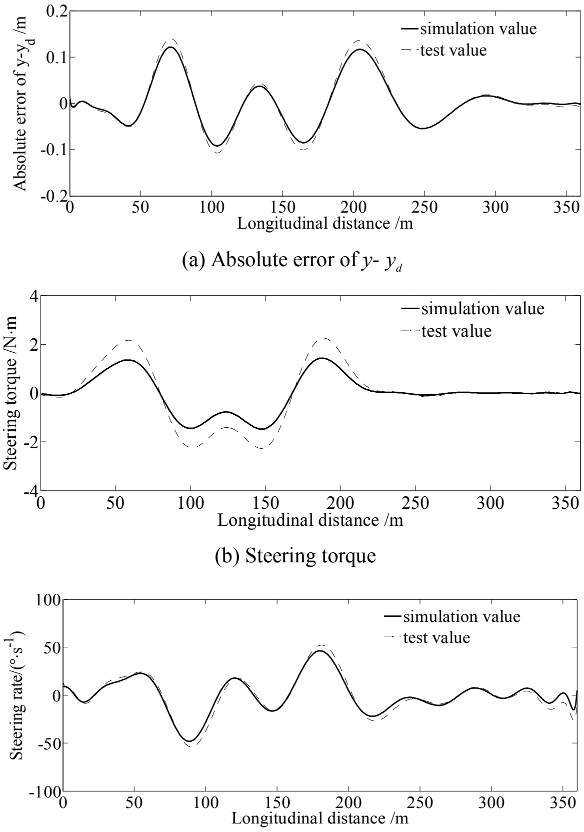

(a) Absolute error of y- y_d

(b) Steering torque

(c) Steering rate

Fig. 9. Comparison of simulation and test value.

5. Conclusions

In this paper, the path-tracking scenario is analyzed, while using the Gauss pseudospectral method, to identify steering torque input for driving a desired path. Accordingly, a 4-DOF simplified vehicle model is used to describe the motion of the vehicle. Then, the problem of the path-tracking maneuver is formulated as a nonlinear programming problem by GPM. Finally, the optimal control problem is solved via SQP method. The calculation accuracy of GPM is evaluated by comparing with the numerical integration algorithm. Simulation results, which are verified to be correct with test driving a vehicle, show that the maximum value of the absolute error between the optimal trajectory and the prescribed trajectory is about 0.12 m. This indicates the errors through the optimal control are small. Furthermore, the results obtained in this paper demonstrate the viability of the Gauss pseudospectral method as a means of obtaining accurate solutions to path tracking optimal control problem.

The trajectory design is an important factor drafting control laws for lane changes in the future. The solution to the path tracking optimal control problem provides valuable insight into the lane changes design work.

Acknowledgment

This research was supported by the Science and Technology Program Foundation of Weifang under Grant 2015GX007. The first author gratefully acknowledges the support agency.

References

[1] K. Wongun, K. Dongwook and Y. Kyongsu, Development of a path-tracking control system based on model predictive control using infrastructure sensors, *Vehicle System Dynamics*, 50 (6) (2012) 1001-1023.

[2] T. Siavash, R. Subhash and H. Henry, Influence of human driving characteristics on path tracking performance of vehicle, *Intelligent Robotics and Applications - Proceedings of the 5th International Conference,* Montreal, Canada (2012) 207-216.

[3] H. Toshihiro, N. Osamu and K. Hiromitsu, Automatic path-tracking controller of a four-wheel steering vehicle, *Vehicle System Dynamics*, 47 (10) (2009) 1205-1227.

[4] D. Bektache, C. Tolba and N. Ghoualmi-Zine, Forecasting approach in VANET based on vehicle kinematics for road safety, *International Journal of Vehicle Safety*, 7 (2) (2014) 147-167.

[5] Y. C. Ju, Robust controller for an autonomous vehicle with look-ahead and look-down information, *Journal of Mechanical Science and Technology*, 25 (10) (2011) 2467-2474.

[6] E. Kim, J. Kim and M. Sunwoo, Model predictive control strategy for smooth path tracking of autonomous vehicle with steering actuator dynamics, *International Journal of Automotive Technology*, 15 (7) (2014) 1155-1164.

[7] S. Taehyun, A. Ganesh and Y. Hongliang, Autonomous vehicle collision avoidance system using path planning and model-predictive-control-based active front steering and wheel torque control, *Journal of Automobile Engineering*, 226 (6) (2012) 767-778.

[8] Y. W. Xu, X. B. Cao and T. Li, Extended Kalman filter based pedestrian localization for collision avoidance, *IEEE International Conference on Mechatronics and Automation,* Chang Chun, China (2009) 805-817.

[9] S. J. Anderson, S. C. Peters and T. E. Pilutti, Semi-autonomous avoidance of moving hazards for passenger vehicles, *ASME 2010 Dynamic Systems and Control Conference*, Cambridge, Massachusetts, USA (2010) 141-148.

[10] A. J. Amir, B. K. Mohsen and K. Reza, Simultaneous vehicle-handling and path-tracking improvement using adaptive dynamic surface control via a steer-by-wire system, *Proceedings of the Institution of Mechanical Engineers, Part D: Journal of Automobile Engineering*, 227 (3) (2013) 345-360.

[11] B. Xu, D. J. Stilwell and A. J. Kurdila, A receding horizon controller for motion planning in the presence of moving obstacles, *2010 IEEE International Conference on Robotics and Automation Anchorage Convention District,* Anchorage, AK (2010) 974-980.

[12] A. Ghaffari, A. Khodayari and S. Arivin, An ANFIS design for prediction of future state of a vehicle in lane change behavior, *2011 IEEE International Conference on Control System, Computing and Engineering,* Penang, Malaysia (2011) 156-161.

[13] S. Jin, Z. Y. Huang and P. F. Tao, Car-following theory of steady-state traffic flow using time-to-collision, *Journal of Zhejiang University-SCIENCE A (Applied Physics & Engineering)*, 12 (8) (2011) 645-654.

[14] D. A. Benson, G. T. Huntington and T. P. Thorvaldsen, Direct trajectory optimization and costate estimation via an orthogonal collocation method, *Journal of Guidance, Control, and Dynamics*, 29 (6) (2006) 1435-1440.

[15] G. W. Reddien, Collocation at a discretization in optimal control, *SIAM Journal of Control and Optimization*, 17 (2) (1979) 298-306.

[16] G. T. Huntington, *Advancement and Analysis of A Gauss Pseudospectral Transcription for Optimal Control*, Massachusetts, USA (2007).

[17] E. M. Yong, L. Chen and G. G. Tang, A survey of numerical methods for trajectory optimization of spacecraft, *Journal of Astronautics*, 29 (2) (2008) 397-406 (in Chinese).

[18] Z. L. Jin, J. S. Weng and H. Y. Hu, Rollover stability of a vehicle during critical driving maneuvers, *Proc. IMechE, Part D: J. Automobile Engineering*, 221 (9) (2007) 1041-1049.

[19] L. X. Zhang, Y. Q. Zhao and G. X. Song, Research on inverse dynamics of vehicle minimum time maneuver problem, *China Mechanical Engineering*, 18 (21) (2007) 2628-2632 (in Chinese).

[20] I. M. Ross and F. Fahroo, Pseudospectral knotting methods for solving nonsmooth optimal control problems, *Journal of Guidance Control and Dynamics*, 27 (3) (2004) 397-405.

[21] E. G. Philip, SNOPT: An SQP algorithm for large-scale constrained optimization, *SIAM Review*, 47 (1) (2005) 99-131.

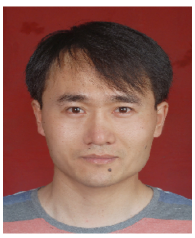

Yingjie Liu obtained his B.S. and M.S. at the Shandong University of Technology, China, in 2007 and 2010, respectively. He later received his Ph.D. degree in 2014 from Nanjing University of Aeronautics and Astronautics, China. He is currently a lecturer at School of Mechanical-Electronic and Vehicle Engineering, Weifang University, China. His current research interests include vehicle system dynamics and control theory on ground vehicles.